Calculations of pH-Dependent Binding of Proteins to Biological Membranes

Maja Mihajlovic and Themis Lazaridis*

Department of Chemistry, City College of the City University of New York, New York, New York 10031

Received: October 15, 2005; In Final Form: December 8, 2005

Binding of proteins to membranes is often accompanied by titration of ionizable residues and is, therefore, dependent on pH. We present a theoretical treatment and computational approach for predicting absolute, pH-dependent membrane binding free energies. The standard free energy of binding, ΔG, is defined as $-RT \ln(P_b/P_f)$, where P_b and P_f are the amounts of bound and free protein. The apparent pK_a of binding is the pH value at which P_b and P_f are equal. Proteins bind to the membrane in the pH range where ΔG is negative. The components of the binding free energy are (a) the free energy cost of ionization state changes (ΔG_{ion}), (b) the effective energy of transfer from solvent to the membrane surface, (c) the translational/rotational entropy cost of binding, and (d) an ideal entropy term that depends on the relative volume of the bound and free state and therefore depends on lipid concentration. Calculation of the first term requires determination of pK_a values in solvent and on the membrane surface. All energies required by the method are obtained from molecular dynamics trajectories on an implicit membrane (IMM1-GC). The method is tested on pentalysine and the helical peptide VEEKS, derived from the membrane-binding domain of phosphocholine cytidylyltransferase. The agreement between the measured and the calculated free energies of binding of pentalysine is good. The extent of membrane binding of VEEKS is, however, underestimated compared to experiment. Calculations of the interaction energy between two VEEKS helices on the membrane suggest that the discrepancy is mainly due to the neglect of protein−protein interactions on the membrane surface.

Introduction

Biological processes such as blood coagulation, cell signaling, immune response, and membrane trafficking involve interactions between proteins and membranes. Vitamin-K-dependent proteins, for instance, interact in a calcium-dependent fashion with cell membranes containing anionic lipids, such as phosphatidylserine (PS), and play a role in blood coagulation.[1,2] Annexin V also associates with negatively charged phospholipids in the presence of Ca^{2+} ions but acts as an anticoagulant, inhibiting the binding of coagulant factors to PS, and promotes apoptosis.[3] Synaptotagmin I, the C2A domain of which associates peripherally with anionic membranes, is believed to serve as a calcium ion sensor for regulated exocytosis from neurons and neuroendocrine cells.[4] Proteins, such as amoebapores and NK-lysin,[5] granulysin,[6] magainins,[7,8] and nisin Z,[9] exert their antibacterial functions by increasing the permeability of the microbial target membrane. The Phox domain of a variety of peripheral proteins, including Mvp1p, Vps5p, Grd19p, and sorting nexins, specifically binds to phosphatidylinositol phopholipids and has a role in membrane trafficking.[10,11]

Biological membranes are often negatively charged and interact strongly with titratable residues, shifting their pK_a. This makes membrane binding pH-dependent. For example, hisactophilin I and II, the actin-binding histidine-rich proteins that contain a myristoyl moeity, bind reversibly to the plasma membrane.[12] At pH > 7.5 the proteins reside in the cytoplasm, whereas at pH = 6.5, at which the cluster of histidine residues arranged around the myristoyl chain is positively charged, the proteins bind to anionic membranes by embedding the myristoyl moeity into the membranes.[13] Binding is of a hydrophobic nature, but it is augmented by electrostatic interactions between cationic histidines and anionic membranes. Saposin C, a lysosomal glycoprotein that serves as a sphingolipid activator,[14−16] also binds to anionic membranes at acidic pH, with binding mediated by protonation of negatively charged residues at the protein surface.[17] Recently, in a computational study, Bollinger et al. predicted that binding of secreted phospholipase A_2 from bee venom to PS-containing vesicles is accompanied by protonation of glutamates near the membrane surface.[18]

Predicting the ionization state of a residue requires knowledge of the pK_a value, i.e., the pH value at which the residue is half-protonated. Since Warshel performed the first pK_a calculations in soluble proteins,[19] several theoretical approaches have been developed.[20−30] Methods based on solving the Poisson−Boltzmann equation (PBE) have been systematically studied and improved.[31−36] The PBE-based calculations are reliable but are usually performed for fixed conformations of proteins and can be computationally costly if combined with molecular dynamics (MD). Multiconformation continuum electrostatics[37] (MCCE) combines the PBE with Monte Carlo sampling for side chain ionization and conformation. The generalized Born approximation[38] is another commonly used method. Yet other approaches combine MD simulations with free energy calculations to account for conformational changes due to titration.[39−42] The past several years have witnessed a number of constant pH molecular dynamics methods[30,43−46] that can predict pK_a values and model pH-dependent phenomena in bulk solvent. None of them has yet been adapted to membrane systems.

Membrane binding is somewhat akin to protein−ligand binding. The calculation of pH-dependent free binding energies has been of interest to several groups. Sharp[47] calculated the electrostatic, nonpolar, and conformational entropy contributions to the change in free energy of binding of hen egg white

* Author to whom correspondence should be addressed. E-mail: tlazaridis@ccny.cuny.edu.

10.1021/jp055906b CCC: $33.50
Published on Web 02/02/2006

lysozyme to the HyHel-10 antibody produced by point mutations as well as pK_a shifts involved. Misra et al.[48] computed the pK_a shifts of ionizable residues upon binding of the λcI repressor to DNA and the contribution of electrostatic energy to the binding. Alexov[49] calculated the uptake/release of protons due to association of plasmepsin, cathepsin D, and endothiapepsin to pepstatin and the electrostatic and van der Waals contributions to the free energy of binding. All these studies compute relative binding free energies (one pH vs another or mutant vs wild-type) and do not calculate the translational and rotational entropy loss involved in binding.

One goal in our lab is the prediction of the membrane-bound configuration and the binding energy of peripheral membrane proteins. Doing so requires treatment of ionization state changes, which at the same time provides the pH dependence of binding. Here we present an approach based on an implicit membrane model that accounts for the electric charge of biological membranes (IMM1-GC). The method involves the calculation of the pK_a values of ionizable groups in solvent and near the membrane, the free energy required for the change in ionization states at a given pH, the effective energy of transfer from solvent to the membrane surface, and the translational/rotational entropy loss upon binding. Thus, this method provides absolute binding free energies.

The method is tested on pentalysine and a helical peptide (VEEKS) that exhibits strong pH-dependent binding to anionic membranes. VEEKS corresponds to residues 256−288 of the α-isoform of rat phosphocholine cytidylyltransferase (CTP).[50,51] The α-helix is highly amphipathic. On the one side of the hydrophobic face there is a cluster of cationic lysine residues, and on the other a mixture of anionic and cationic residues. The net charge of VEEKS at neutral pH is −2 (assuming that all ionizable residues adopt their standard ionization states), with nine negatively charged and seven positively charged residues. Still, it binds negatively charged membranes due to the positioning of the charges. The lysine residues are key to membrane binding, as confirmed by fluorescence and circular dichroism (CD) measurements on mutant peptides.[52] The authors showed that the substitution of the three interfacial glutamates (Glu257, Glu268, and Glu279) with glutamines promotes membrane binding and eliminates the pH dependence for binding. They further suggested that the three glutamates are likely protonated (though they did not measure the pK_a values) adjacent to anionic, but not zwitterionic membranes, and that this dictates, in part, the selectivity of the peptide/protein for anionic membranes. The measured apparent pK_a of binding of the wild-type protein to small unilamellar vesicles (SUVs) was found to increase from 4.3 to 5.9 as the anionic fraction increased from 0 to 35 mol %.

Methods

Implicit Membrane Model. Molecular dynamics simulations were carried out using the program CHARMM.[53] The effective energy of a protein solute in a lipid membrane is obtained using IMM1-GC as described previously.[54] Briefly, the effective energy is calculated as the sum of the intramolecular energy of the solute, as implemented in the CHARMM polar hydrogen force field,[55] the implicit solvation free energy that describes the interaction of each atom with the solvent, and the electrostatic interaction energy between the lipid headgroups and the solute. The last energy term (henceforth referred to as the GC term) is obtained from the Gouy−Chapman theory for the electrical double layer,[56] which gives the electrostatic interaction potential as a function of distance from a uniformly charged membrane. The membrane is taken to be parallel to the *xy*-plane, with its center located at $z = 0$. The plane of smeared charge is taken to be 3 Å outward from the nonpolar/polar interface.

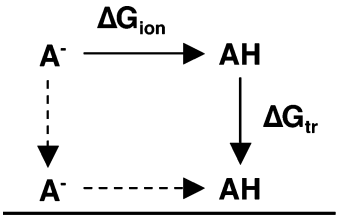

Figure 1. Thermodynamic cycle for membrane binding. The upper right path is used in this work. The first step is the change in ionization state to match that prevailing on the membrane surface. The second step is the transfer from solvent to the membrane at constant ionization state. The horizontal lines depict the membrane.

Thermodynamic Cycle for Membrane Binding. The negative surface charge of the membrane gives rise to a higher concentration of H^+ ions near the anionic membrane than in the bulk. For ideal solutions pH is defined as $-\log [H^+]$. However, for nonideal solutions, such as those considered here, pH should be defined using the hydrogen ion activity instead of its concentration, $pH = -\log a_{H^+}$. Since the activity (or equivalently the chemical potential) is the same everywhere in a system at equilibrium, pH is also the same everywhere in the system. Loosely speaking, there are more H^+ ions near the membrane, but they are interacting favorably with the membrane charge, so they are as "available" near the membrane as they are in the bulk.

Membrane binding can be represented by the thermodynamic cycle of Figure 1. In the first step, all titratable residues change their ionization state from that prevailing in solution to that prevailing on the membrane. In the second step, the protein is transferred from solution to the membrane surface. ΔG_{ion} is the free energy of the first step, and ΔG_{tr} is the transfer free energy. The latter consists of the effective energy of transfer (ΔW_{tr}) and the translational/rotational entropy contribution. ΔG_{ion} and ΔW_{tr} depend on pH. The sum, $\Delta G = \Delta G_{ion} + \Delta G_{tr}$, characterizes pH-dependent binding of the protein to membranes. The protein binds to membranes at the pH range at which the sum is negative. $\Delta G = 0$ corresponds to equal amounts of membrane-bound and free protein, and the pH value at which this is achieved is equal to the apparent pK_a of binding.

Calculation of ΔG_{ion} requires knowledge of the ionization states of titratable residues of the protein in solvent and near the membrane at a given pH, and thus their pK_a values. Since membrane binding of VEEKS takes place at pH 4.00−7.50,[52] we assume that only the side chains of glutamic and aspartic acids are titratable and that the side chains of lysines and arginines are always protonated (there are no histidines). This assumption can be relaxed for other systems. The pK_a values of the isolated glutamic and aspartic acids in solvent are assumed to be 4.3 and 3.9.[57] The pK_a values of these residues in proteins in solvent and upon their binding to the membrane can be significantly shifted from the values of isolated residues. The pK_a shifts in solvent depend on electrostatic interactions with other ionizable groups, hydrogen bonding with nonionizable groups, and the degree of exposure of the residues to the solvent. In addition to these effects, the membrane environment gives rise to shifts in pK_a values through the change in solvent environment and, in the case of charged membranes, through

electrostatic interactions between charged residues and the membrane surface charge.

pK_a Calculations. An ionization state k of a protein with N titratable residues can be described by a vector $\mathbf{x}^k = (x_1^k, x_2^k, ..., x_N^k)$, where x_i^k is equal to 1 or 0, depending on whether the group i is deprotonated or protonated, respectively. The total number of possible ionization states of the protein is $\Omega = 2^N$. The probability (or occupancy) of each ionization state, $P(\mathbf{x}^k)$, is

$$P(\mathbf{x}^k) = [\exp(-\beta G(\mathbf{x}^k))]/\{\sum_{\omega=0}^{\Omega-1} [\exp(-\beta G(\mathbf{x}^\omega))]\} \quad (1)$$

where $\beta = 1/RT$ (R is the universal gas constant and T is the temperature) and $G(\mathbf{x}^k)$ is the free energy of ionization state k. After defining the ionization state at which all residues are protonated as the reference state, $\mathbf{x}^0$, eq 1 can be expressed as

$$P(\mathbf{x}^k) = [\exp(-\beta \Delta G^k)]/\{1 + \sum_{\omega=1}^{\Omega-1} [\exp(-\beta \Delta G^\omega)]\} \quad (2)$$

The total free energy of ionization, ΔG^k, accounts for the ionization of one or more residues necessary to obtain state k from 0.

Because classical force fields cannot provide the absolute free energy of protonation, we calculate shifts in pK_a due to the protein and/or membrane environment using an implicit solvation model (EEF1.1[58,59] in water, IMM1-GC on the membrane). The difference in free energy of protonation is approximated by the difference in effective energy change upon protonation. The free energy of ionization is given by

$$\Delta G^k = -2.303RT \sum_{i=1}^{N} x_i^k(\mathrm{pH} - \mathrm{p}K_{a,i}) + [W(\mathbf{x}^k) - W(\mathbf{x}^0) - \sum_{i=1}^{N} x_i^k \Delta W_{i,\mathrm{model}}] \quad (3)$$

The first term is the protonation free energy for the fully solvent-exposed residue. The term in brackets is the shift in protonation free energy due to the protein environment. $W(\mathbf{x}^k) - W(\mathbf{x}^0)$ is the change in effective energy between states k and 0. $\Delta W_{i,\mathrm{model}}$ is the same in a model compound where residue i is fully exposed to solvent (see below). All effective energies are obtained from MD. In eq 3 only the first term on the right-hand side depends explicitly on pH; the term in brackets does not depend on pH but depends on a given state.

The probability of state k is obtained by substituting eq 3 into eq 2. The probability of residue i to be deprotonated is then

$$p(x_i) = \sum_{k=0}^{\Omega-1} x_i^k P(\mathbf{x}^k) \quad (4)$$

This probability plotted versus pH defines the titration curve. The pK_a value of the residue i in a given environment is found from the titration curve as the pH value at which the residue is half-ionized. The pK_a calculation method was validated on turkey ovomucoid third domain (Supporting Information).

Membrane Binding Free Energy. The negative membrane charge is expected to shift the pK_a of acidic residues to higher values than those in solution. Therefore, membrane binding at acidic pH will be accompanied by protonation of such residues. The free energy of protonation of residues as a function of pH can be estimated as

$$\Delta G_{\mathrm{ion}}(\mathrm{pH}) = RT \sum_{i=1}^{N} [2.303(f_{\mathrm{AH},i,\mathrm{membrane}} - f_{\mathrm{AH},i,\mathrm{solvent}})(\mathrm{pH} - \mathrm{p}K_{a,i,\mathrm{solvent}}) + (f_{\mathrm{AH},i,\mathrm{membrane}} \ln f_{\mathrm{AH},i,\mathrm{membrane}} + f_{\mathrm{A}^-,i,\mathrm{membrane}} \ln f_{\mathrm{A}^-,i,\mathrm{membrane}}) - (f_{\mathrm{AH},i,\mathrm{solvent}} \ln f_{\mathrm{AH},i,\mathrm{solvent}} + f_{\mathrm{A}^-,i,\mathrm{solvent}} \ln f_{\mathrm{A}^-,i,\mathrm{solvent}})] \quad (5)$$

where $f_{\mathrm{AH},i,\mathrm{membrane}}$ and $f_{\mathrm{AH},i,\mathrm{solvent}}$ are the protonation fractions of residue i near the membrane and in solvent, respectively, and $f_{\mathrm{A}^-,i,\mathrm{membrane}} = (1 - f_{\mathrm{AH},i,\ \mathrm{membrane}})$ and $f_{\mathrm{A}^-,i,\mathrm{solvent}} = (1 - f_{\mathrm{AH},i,\mathrm{solvent}})$ are the fractions of deprotonated residue i near the membrane and in solvent. The protonation fraction in a given environment is

$$f_{\mathrm{AH},i,\mathrm{env}} = 1 - p(x_i)_{\mathrm{env}} \quad (6)$$

where $p(x_i)_{\mathrm{env}}$ is defined by eq 4. The first term on the right-hand side of eq 5 is the standard free energy of the reaction $\mathrm{A}^- \rightarrow \mathrm{AH}$. The remaining terms are the ideal entropic contributions arising from concentration changes.

The effective energy of transfer to the membrane depends on the residue ionization states and is therefore pH-dependent. In principle, one should calculate ΔW_{tr} for each ionization state and average the results. For convenience, we developed an alternative approach where titratable residues are represented as hybrids between the protonated and deprotonated versions. That is, partial charges, geometric parameters (angle, bond, and dihedral parameters), and nonbonded van der Waals and solvation parameters of selected atoms are linearly interpolated between the corresponding values for the protonated and deprotonated versions. The new partial charges are assigned to the selected atoms in the topology file: the CB, CG, OD1, OD2, and HD2 atoms of aspartic acid and the CG, CD, OE1, OE2, and HE2 atoms of glutamic acid. Geometric and solvation parameters involving these atoms are also modified. Titratable hydrogens are present in both the protonated and the deprotonated form of a residue, but their partial charges are set to zero in the deprotonated form. The well depth (ϵ in the van der Waals parameters) of titratable hydrogen is interpolated between its value for the fully protonated form and zero. The radius of the hydrogen is however kept constant.

The pH-dependent transfer effective energy is calculated from

$$\Delta W_{\mathrm{tr}}(\mathrm{pH}) = W_{\mathrm{membrane}}(\mathrm{pH}) - W_{\mathrm{solvent}}(\mathrm{pH}) \quad (7)$$

where W_{membrane} and W_{solvent} are the average effective energies of the protein near the membrane and in solvent, respectively. This term incorporates all hydrophobic and electrostatic effects. These energies are extracted from MD trajectories. The partial charges of each residue are set according to their protonation fractions at the pH of interest.

Binding of proteins to membranes incurs a loss of translational and rotational degrees of freedom. The translational and rotational entropy loss for pentalysine adsorption onto an anionic membrane, on the molarity scale, was estimated by Ben-Tal et al.[60] Their standard free energy, $\Delta G^\ominus$, was defined as $-RT \ln(C_b/C_f)$, where C_b and C_f are the molarities of bound and free protein, whereas ours $\Delta G = -RT \ln(P_b/P_f)$, where P_b and P_f are the *total amounts* of bound and free protein. Therefore, they differ by $RT \ln(V_b/V_f)$, where V_b and V_f are the volumes available to bound and free protein, respectively. Our standard free energy and apparent pK_a depend on the amount of lipid present; as lipid concentration increases, the translational entropy cost

decreases and free energy becomes more negative. The amounts of bound and free protein are defined with respect to the total volume of the solution ($V = V_b + V_f$). The standard free energy of binding is thus

$$\Delta G = -RT \ln(P_b/P_f) = -RT \ln(C_b/C_f) - RT \ln(V_b/V_f) \quad (8)$$

If lipid concentration is low, $V_b \ll V$, then the volume available to free protein per liter of solution is $V_f \approx V = 1.00 \times 10^{27}$ Å^3. V_b can be calculated as

$$V_b = [L] N_A a_o \lambda \quad (9)$$

where [L] is the accessible lipid concentration (in M), N_A is Avogadro's number, a_o is the area per lipid, and λ is a distance from the membrane that defines the membrane-bound state. For λ we use the value 14.25 Å suggested by Ben-Tal et al.;[60] the results are not sensitive to small variations in λ. The standard transfer free energy can be expressed as

$$\Delta G_{tr} = \Delta W_{tr} - RT \ln(V_b/V_f) - T\Delta S^{\Theta} \quad (10)$$

where ΔS^{Θ} is the translational and rotational entropy change, calculated by Ben-Tal et al. The standard free energy of binding is

$$\Delta G = \Delta G_{ion} + \Delta G_{tr} \quad (11)$$

The apparent pK_a of binding is the pH at which $P_b = P_f$, or $\Delta G = 0$.

Simulation Protocols. In IMM1-GC, the membrane is considered to be parallel to the *xy*-plane, with its center located at $z = 0$. The thickness of the hydrocarbon core of the membrane was 26 Å, with an area of 70 Å^2 per lipid. With these parameters, the hydrophobic/hydrophilic interface is at $z = \pm 13$ Å and the smeared charge is at $z = \pm 16$ Å. The valence of the lipids was 1. For pentalysine, the membrane contained different ratios of phosphatidylcholine (PC)/PS in a 0.1 M monovalent solution, at $T = 298$ K.[61] In the case of VEEKS, the molar fraction of anionic lipids (corresponding to the phosphatidylglycerol (PG)/PC mixture) was 0.35, and the salt concentration was 0.131 M, or in the case of transfer energy 0.022 M. All simulations were performed at $T = 293$ K. The simulation conditions correspond to those in experiment.[52] All energy minimizations were done using the adopted basis Newton−Raphson algorithm (ABNR) for 300 steps, and the numerical integration of equations of motion was carried out using the Verlet integrator (unless otherwise noted) with a time step of 2 fs. For the MD simulations all bonds involving hydrogen atoms were fixed using SHAKE constraints.

Initial Structures. Pentalysine (Ac-KKKKK-NH_2) was built in an extended conformation and placed on the membrane surface, its center of mass at $z = 17$ Å and side chains parallel to the surface. Since experiments were carried out at pH = 7.0,[61] all lysine residues were protonated.

VEEKS was built as an ideal α-helix ($\phi = -57°$, $\psi = -47°$), the sequence of which corresponds to residues 256−288 of domain M of phosphocholine cytidylyltransferase and is VEEKSKEFVQKVEEKSIDLIQKWEEKSREFIGS. Since the peptide was acetylated and aminated at its N- and C-termini,[52] the helix was blocked using acetyl and methylamide residues. For simulations near the membrane, VEEKS was placed in the preferred orientation relative to the membrane (see below).

Determination of the Optimal Orientation of VEEKS. Four simulations were run starting from an ideal α-helix at four arbitrary orientations obtained by rotating the helix 90° around its axis. VEEKS, in each of the four orientations, with all Glu and Asp residues protonated, was placed in the vicinity of the membrane, and its energy was minimized. A 100 ps equilibration at the given temperature was followed by a 600 ps MD simulation. The energy of the last structure after 700 ps was minimized. The minimized energies of VEEKS in the four orientations were compared; the lowest corresponded to the preferred orientation. All subsequent simulations near the membrane were run starting from VEEKS oriented in the optimal orientation, which is assumed to be independent of pH.

pK_a Calculations. The initial structure of VEEKS, with all Glu and Asp residues protonated or deprotonated, was placed in the vicinity of the membrane or in solvent, respectively. Prior to MD simulations, the following test was run to determine which carboxyl oxygen of Glu and Asp should be protonated: The energy of the structure was minimized; one of the two carboxyl oxygens of a residue was protonated at a time; the energies of the two structures were compared. The state that gave the lower energy was selected. The energy of the protonated structure was minimized, followed by a 150 ps equilibration.

There are nine acidic residues in VEEKS, each of which can be protonated or deprotonated. The number of possible protonation states is $2^9 = 512$. However, given that in IMM1-GC both van der Waals and electrostatic interactions are cut off at 9 Å, residues located more than 9 Å away from a titratable residue do not affect its protonation state. Thus, for each ionizable residue, only its neighbors within a 9 Å radius were considered. The more distant residues are kept in their initial ionization states (deprotonated in solvent, protonated near the membrane). If, for example, the target residue has two ionizable neighbors within 9 Å, then there are eight protonation states, leading to eight MD simulations. Doing this reduces the total number of simulations from 512 in each environment to 92 in solvent and to 88 near the membrane.

For each protonation state the energy of the structure was minimized. The CONS FIX facility in CHARMM was used to rigidly fix all residues beyond 9 Å. This makes longer simulation times accessible and significantly improves precision by reducing the energy fluctuations caused by residues far from the target residue. Each simulation was run for 1 ns, during which coordinates were collected every 0.2 ps. The Nosé−Hoover[62,63] thermostat was used in these simulations to ensure constant temperature. All energies were averaged over 5000 frames.

MD simulations of pentapeptides (AAXAA, where X is E or D) in an extended conformation, with the N and C termini blocked, were used to obtain the effective energy change upon protonation of the fully solvent-exposed residues (ΔW_{model} in eq 3). Prior to MD simulations, the energy of the conformation was minimized and the CONS FIX facility was applied to all residues except the titratable group. The structure was equilibrated at the given temperature for 150 ps, and then the production stage was run for 3.2 ns, using the Nosé−Hoover thermostat. All energies were averaged over 16 000 frames.

Transfer Energy Simulations. The energy of the initial structure of pentalysine was minimized, followed by a 20 ps simulation with harmonic constraints on the backbone atoms, followed by a 1 ns unconstrained MD simulation. The energy of pentalysine in solvent was obtained by transferring the protein from the membrane to solvent. All energies were averaged over 900 ps (or 4500 frames).

The initial structure of VEEKS, with the predetermined protonation state of Glu and Asp residues that depends on pH, was placed in the vicinity of the membrane, with its center of

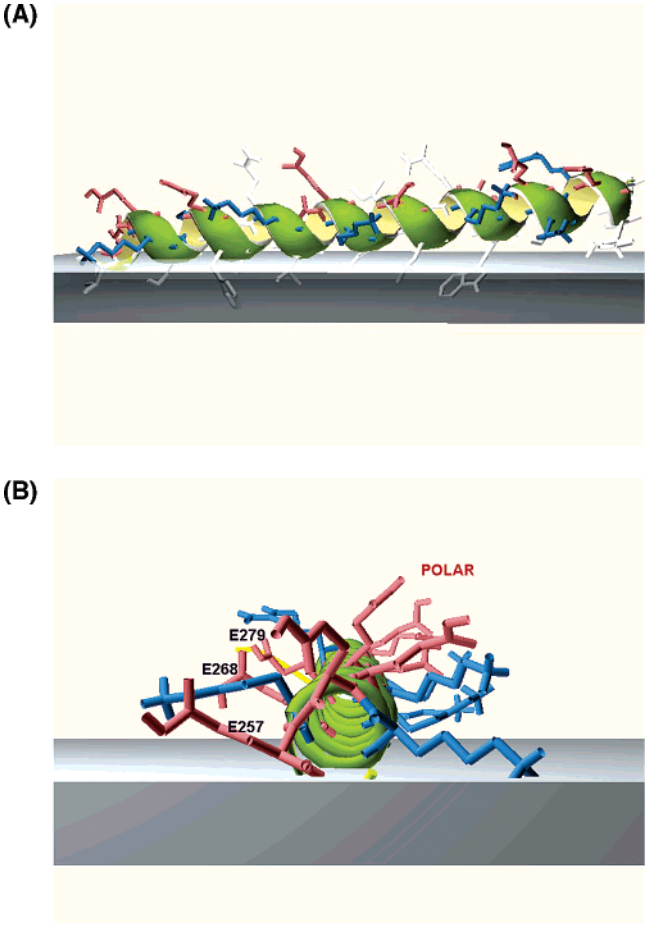

Figure 2. (A) Lowest energy conformation of VEEKS after 700 ps MD simulation and energy minimization. All Glu and Asp residues are protonated. The upper surface represents the charge plane. The lower surface represents the hydrocarbon/headgroup interface. Acidic residues are shown in red and basic residues in blue. (B) The front view. Glu257, Glu268, and Glu279 are located at the polar−nonpolar interface. Other glutamates and an aspartate are positioned in the polar face. The nonpolar face is inserted into the membrane.

mass at $z = 17.5$ Å and in the optimal orientation, and its energy was minimized. The miscellaneous mean-field potential (MMFP) facility of CHARMM was used to restrain the backbone of VEEKS from exiting a cylinder of 30.25 Å radius (with the axis of the cylinder along the *x*-axis). A 100 ps MD simulation with harmonic constraints on the backbone atoms was followed by a 600 ps unconstrained MD simulation. The simulations were performed from pH 1.0 to 9.0, in steps of 1.0 pH units. The simulations were repeated using two extra sets of random numbers. Atomic coordinates were saved, and energies were calculated after every 100 steps. All energies were first averaged over 3000 frames and then over the three seeds. To estimate the energy of the protein in solvent, at each frame, the protein was transferred, along the *z*-axis, from the membrane to solvent keeping the conformation the same to minimize statistical error; its energy was calculated and averaged over all frames and seed numbers.

Results

Optimal Orientation. The lowest effective energy orientation of VEEKS is shown in Figure 2. The conformation corresponds to the last structure after 700 ps of simulation and minimization. Its energy (with all Glu and Asp residues protonated) is by 10−14 kcal/mol lower than that of the other three orientations and

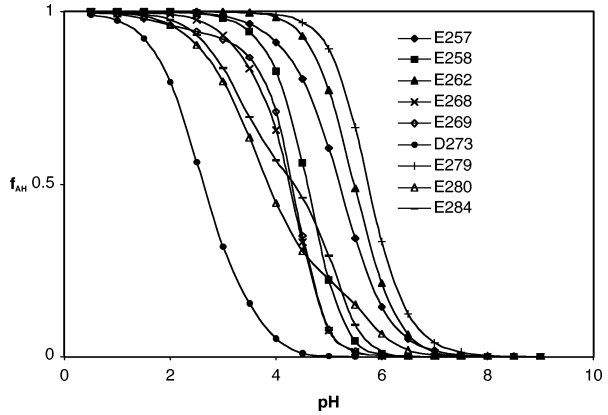

Figure 3. Titration curves for Glu and Asp residues of VEEKS in solvent.

is about 6 kcal/mol lower than that of the same conformation in water. The GC term is about −8 kcal/mol. The stabilization of the protein upon binding to the membrane is mainly due to favorable interactions between the protein and the negative surface charge of the membrane. The six lysine residues and an arginine are within one Debye length (κ^{-1} is about 9 Å for a 0.131 M monovalent salt solution) and interact electrostatically with the negative surface charge. The hydrophobic residues, Phe263 and Trp278, have their side chain atoms slightly intercalated into the lipid core. The center of mass of the protein is located at $z = 19$ Å. The orientation is consistent with experiment.[64,65] However, the extent of penetration of Trp278 into the hydrocarbon core predicted by our study (∼1 Å below the headgroup/hydrocarbon boundary) is much smaller than that measured by fluorescence quenching by a brominated lipid. Johnson and Cornell measured that the tryptophan intercalates near the 9,10-positions of the fatty acyl chain, or ∼6 Å below the hydrophilic/hydrophobic interface.[64] This discrepancy could be due to differences in the geometry of vesicles used in the studies. SUVs were used in the fluorescence measurements, while a planar bilayer, which is a good approximation for large unilamellar vesicles (LUVs), was used in simulations. The cohesive forces between lipid molecules in SUVs are weaker and less disrupted by binding of proteins and/or intercalation of hydrophobic residues into the hydrocarbon core than those in well-packed LUVs. As a consequence, proteins bind more strongly to SUVs than to LUVs.[66−69] Experiments performed on lipid bilayers or LUVs would help to resolve this issue.

The front view of VEEKS bound to the membrane is shown in Figure 2B. Three interfacial glutamic acids, Glu257, Glu268, and Glu279, are positioned at the periphery of the nonpolar face, with their center of mass 4.0−7.0 Å above the hydrophobic/hydrophilic boundary. Other glutamates are located in the polar face of the helix, away from the membrane. Such an arrangement is in agreement with the experimental study of peptides derived from domain M of CTP interacting with sodium dodecyl sulfate[65] and is essential for binding.[52]

pK_a Values of Titratable Residues. The pK_a values of glutamic and aspartic acid residues were estimated from titration curves, obtained by plotting the probability of residue *i* to be protonated (eqs 4 and 6) vs pH. The titration curves in solvent are shown in Figure 3. Titration of most residues follows the Henderson−Hasselbach (HH) equation: Residues are protonated at low pH, abruptly change protonation state over a narrow pH range, and are deprotonated at higher pH. However, Glu280 and Glu284 show a somewhat irregular behavior. Glu280 has three titratable neighbors: Asp273, Glu279, and Glu284. Asp273 is essentially deprotonated at pH values above 2.6. As

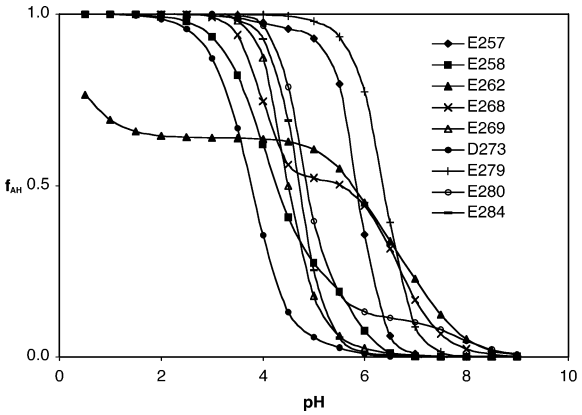

Figure 4. Titration curves for Glu and Asp residues of VEEKS near the anionic membrane.

pH increases, both Glu280 (pK_a = 3.8) and Glu284 (pK_a = 4.3) continue to deprotonate, which gives rise to repulsive interactions among the residues. The effect of the repulsive interactions is to delay deprotonation of Glu280, seen as the broadening of the transition region. The pK_a value of Glu280 is, however, surprisingly low, given the environment. A closer inspection of MD trajectories reveals that deprotonated Glu280 makes an occasional salt bridge with the NZ atom of Lys277 and a more persistent salt bridge with the NH1 atom of Arg283. The ion pairing stabilizes the deprotonated form of Glu280 and lowers its pK_a value. At pH ~5.0, Glu279 begins to change its ionization state as well, which further accentuates the irregular shape of the titration curve. The pK_a values of the interfacial glutamates, Glu257, Glu268, and Glu279, are 5.2, 4.3, and 5.7, respectively.

The titration curves of glutamates and an aspartate near the membrane are shown in Figure 4. The residues stay protonated over a wider pH range as compared to that in solvent. This is due primarily to the negative charge of the membrane surface. Noticeably, more residues exhibit non-HH behavior near the membrane. Titration of Glu262 is a case in point. The residue has a pK_a value of 5.8, though it is exposed to the solvent not to the membrane. Repulsive interactions with Glu258 (pK_a = 4.3) tend to elevate the pK_a of Glu262, but at the same time, deprotonated Glu262 is stabilized by a salt bridge with the NZ atom of Lys259. These two competing effects produce the leveling off of the titration curve at the low pH range. In solvent, the probabilities of states in which Glu262 is deprotonated are very small so that interactions with Lys259 do not affect the titration of Glu262. Interactions of Phe263 with the protonated Glu262 are preferable to those with the deprotonated residue, especially in solvent. Likely, these interactions are responsible for differences in the titration pattern of Glu262 in solvent and on the membrane.

Glu268, another residue whose titration shows non-HH behavior, has three titratable neighbors in its surroundings: Glu262, Glu269, and Asp273. Its pK_a value is 5.5. The first residue to titrate at pH ~4.0 is Asp273, but its deprotonation does not lead to strong repulsive interactions with other, still mostly protonated residues. The interactions become more substantial at pH ~4.3 as Glu268 and Glu269 are now ~40% and ~50% deprotonated, respectively. Repulsive interactions influence further deprotonation of Glu268 that gets to some extent postponed, seen as the shoulder in the titration curve. At pH values above 5.8, all four residues are deprotonated and repulsive interactions among them broaden the titration curve.

The pK_a values of Glu and Asp residues in solvent and near the membrane are given in Table 1. In solvent, Asp273 and Glu280 have lower pK_a values than the isolated fully solvent-exposed residues. According to MD trajectories, all three residues make salt bridges with basic residues. A consistent ion-pairing partner for Asp273 is the NZ of Lys277, though it occasionally interacts with the NZ of Lys270 as well. As already mentioned, Glu280 interacts with Arg283 and, sometimes, with Lys277. However, the pK_a values of Glu257, Glu262, and Glu279 are significantly elevated due mainly to repulsive electrostatic interactions between acidic residues. The only titratable neighbor of Glu257 is Glu258, the pK_a value of which is 4.6. Repulsive interactions between the deprotonated residues, as well as favorable interactions between the protonated Glu257 and Val256, elevate the pK_a value of Glu257. Unfavorable interactions with Glu258 also raise the pK_a value of Glu262. Though Glu279 has Asp273 and Glu280 in its surroundings, both of which have low pK_a values, 2.6 and 3.8, respectively, its elevated pK_a value is mostly due to interactions between Arg283 and the protonated Glu279 that are by ~2 kcal/mol more favorable than those with the deprotonated Glu279. However, this destabilizing salt bridge could be an artifact due to force field inadequacies (Supporting Information).[70,71]

TABLE 1: pK_a Values of Glu and Asp Residues of VEEKS in Solvent and the Membrane Environment[a]

residue	solvent	membrane
E257	5.2	5.9
E258	4.6	4.3
E262	5.5	5.8
E268	4.3	5.5
E269	4.3	4.5
D273	2.6	3.8
E279	5.7	6.4
E280	3.8	4.9
E284	4.3	4.7

[a] The pK_a values of the isolated Glu and Asp residues are 4.3 and 3.9, respectively.[57]

Near the membrane, the negative charge of the membrane surface and the lower polarity of the medium give rise to pK_a values larger than those in solvent. All GLU and ASP residues of VEEKS experience positive pK_a shifts, except Glu258, which has a pK_a value of 4.6 in solvent, whereas it is 4.3 near the membrane. In the membrane environment, this residue occasionally makes a salt bridge with the NZ atom of Lys261. The salt bridge is not persistent but still brings about a certain degree of stabilization of deprotonated Glu258. Large pK_a shifts of Asp273 and Glu280 are due to the salt bridges (see above) that lower their pK_a values in solvent. These residues are positioned in the polar face of the helix and are extended toward solvent (Figure 2B) and thus do not interact with the membrane. The large pK_a shifts of Glu257, Glu268, and Glu279 upon binding are however related to their position relative to the membrane. As shown in Figure 2B, these residues reside just above the charge plane (1.0−4.0 Å). That environment is less polar than water, which strengthens electrostatic interactions and favors the protonated state. In addition, repulsive interactions between the membrane surface and the negatively charged residues elevate their pK_a values.

Free Energy of Binding of Pentalysine. Victor and Cafiso reported that the partition coefficient for pentalysine bound to the membrane containing 33 mol % phosphatidylserine is K_p = 300 M^{-1}, and thus the free energy of binding $\Delta G_p = -RT \ln K_p = -3.4$ kcal/mol.[61] Their partition coefficient is defined as $K_p = X_b/C_f$, where $X_b = P_b/[L]$ is the mole fraction of the membrane-bound peptide and [L] is the accessible lipid concentration, 0.125M. To compare their free energy with ours, we have to subtract $RT \ln [L]$, $\Delta G = \Delta G_p - RT \ln [L] = -2.2$

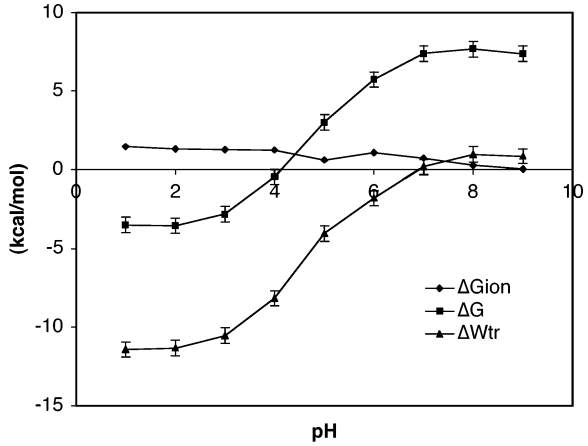

Figure 5. Free energy of protonation (ΔG_{ion}), effective transfer energy (ΔW_{tr}), and free energy of binding (ΔG) as a function of pH. $\Delta G = \Delta G_{ion} + \Delta W_{tr} - RT \ln(V_b/V_f) - T\Delta S^{\Theta}$, where $\Delta W_{tr} = W_{membrane} - W_{solvent}$, $T\Delta S^{\Theta} = -1.9RT$, and $RT \ln(V_b/V_f) = -9.1RT$. Error bars represent the standard deviation of the mean. The salt concentration is 0.022 M, the temperature is 293 K, and the anionic fraction is 0.35. The apparent pK_a of binding is ~4.2.

kcal/mol. Since the experiment is performed at pH = 7.0, we assumed that the lysine residues are protonated both in solvent and on the membrane and thus that $\Delta G_{ion} = 0$. At the given [L], area per lipid of 70 Å^2, and λ = 14.25 Å,[60] the binding volume, V_b, calculated from eq 9, is 7.51×10^{25} Å^3, the volume available to free protein is $V_f \approx V = 1.00 \times 10^{27}$ Å^3, and $-RT \ln(V_b/V_f) = 1.5$ kcal/mol (at $T = 298$ K). The transfer effective energy $\Delta W_{tr} = -3.5 \pm 0.1$ kcal/mol. Given $\Delta S^{\Theta} = -1.9R$,[60] the free energy of binding of pentalysine, calculated from eq 11, is $\Delta G = -0.9 \pm 0.1$ kcal/mol. The slight discrepancy between the measured and the calculated ΔG is likely due to lipid demixing, an effect not captured with our implicit membrane model. Victor and Cafiso's results suggest that the partition coefficient is highly sensitive to the molar fraction of anionic lipids. If the lysine residues induce lipid demixing, then the local lipid concentration will be higher than the average anionic molar percentage. Our ΔG calculated at 50, 66, 80, and 100 mol % of anionic lipids is −1.9, −2.7, −3.2, and −3.6 kcal/mol, respectively. This is sufficient to bring the calculated ΔG close to the experimental result.

pH-Dependent Free Energy of Binding. Johnson et al. reported that the apparent pK_a of binding of VEEKS to SUVs (0.3 mM total lipid concentration) containing 35 mol % of anionic lipids, in a 0.131 M monovalent salt solution, is ~5.9.[52] However our calculations at the same conditions (data not shown) gave an unfavorable free energy of binding at the studied pH range (pH 1.0−9.0). Reasons for this discrepancy are suggested in the Discussion section.

Figure 5 shows the pH dependence of the free energy of protonation (ΔG_{ion}) (diamonds), the transfer effective energy (ΔW_{tr}) (triangles), and the free energy of binding (ΔG) (squares), at 0.022 M salt concentration. Given the accessible lipid concentration of 0.18 mM,[52] area per lipid of 70 Å^2, and λ of 14.25 Å,[60] V_b is 1.08×10^{23} Å^3, V_f is ~1.00×10^{27} Å^3, and thus $-RT \ln(V_b/V_f) = 9.1RT$ (or 5.3 kcal/mol, at $T = 293$ K). ΔS^{Θ} is assumed to be the same as for pentalysine, $-1.9R$.[60] ΔG is computed from eq 11. The transfer effective energy and the free energy of binding curves have sigmoidal shapes: They approach limiting values at low and high pH and gradually increase at medium pH. The pH at which $\Delta G = 0$ defines the apparent pK_a of binding. At 0.022 M ionic strength, its value is ~4.2. The free energy of protonation exhibits it maximum at pH ~6.0 and decreases to 0 at pH ~9.0.

The pH-dependent net charge of VEEKS in solvent and on the membrane, the average position of the center of mass relative to the center of the membrane, and the average GC term at 0.131 and 0.022 M salt concentrations are given in Table 2. The theoretical isoelectric point (pI) of VEEKS, calculated based on standard pK_a values, is 5.0. On the basis of the net charge of VEEKS, the pI is 5.4 in solvent and 6.1 on the membrane. The net charge of the protein decreases as the pH increases from 1.0 to 9.0. At the same time, the center of mass of VEEKS moves away from the membrane and the GC term, which depends on both the net charge and the positions of the atoms, decreases. The anionic headgroups of the membrane are more shielded in the 0.131 M salt solution than in the 0.022 M solution, resulting in displacement of the center of mass at low pH and weaker protein−membrane electrostatic interactions (smaller GC term at low pH). The same shielding, however, produces stronger binding at 0.131 M than at 0.022 M salt concentration at pH values above ~7.0. The net charge of VEEKS is now negative, and the screening of the negative membrane surface charge decreases repulsion between the membrane and the protein.

In the pH range from 1.0 to 3.0, the position of the center of mass of the protein and the GC term are monotonically increasing at 0.022 M salt, as expected. However, at 0.131 M salt they are decreasing and start to increase above pH 3.0. The position of the protein is the result of a balance between protein−membrane and intraprotein interactions. At low salt concentration the protein−membrane interactions are the overriding factor. At high salt, they face competition from intraprotein interactions.

Figure 6 shows the minimized average structure of VEEKS at different pH values. At pH 2.0, nonpolar residues of the helix are positioned below the charge plane, the center of mass of protonated Glu257, Glu268, and Glu279 is located at 18.4, 19.5, and 21.9 Å, respectively, lysine residues interact with the membrane surface, and other acidic residues face solvent. Protonation of the three interfacial glutamates decreases repulsion with the membrane charge and promotes membrane binding. The lysine residues are close enough to the headgroup region and thus favorably interact with the membrane over the entire pH range. Our results hence agree with the hypothesis that protonation of the interfacial glutamates is a prerequisite for binding.[52,65]

Johnson et al. found that the free energy of binding of VEEKS to 35 mol % PG/PC SUVs at 0.022 M salt concentration and pH = 7.0 is approximately −7.7 kcal/mol.[52] Their free energy of binding is defined as $\Delta G = -RT \ln(P_b/P_f) - RT \ln([W]/[L])$, where [W] = 55.5 M is the water concentration and [L] = 0.18 mM is the accessible lipid concentration. To convert the experimental ΔG to our standard state, we subtract $-RT \ln([W]/[L]) = -7.4$ kcal/mol and obtain that ΔG is equal to −0.33 kcal/mol. The ΔG that we computed at the same pH and ionic strength is 7.4 ± 0.5 kcal/mol. As at higher ionic strengths, we significantly underestimate membrane binding affinity.

Discussion

We presented a theoretical treatment and computational approach for the calculation of pH-dependent membrane binding free energies and the apparent binding pK_a. The method utilizes MD with an implicit membrane, IMM1-GC, which accounts for the negatively charged headgroups of the membrane. In this method, (1) all energies are obtained using the same force field,

TABLE 2: Net Charge in Solvent and on the Membrane, the Average Position of the Center of Mass of VEEKS, and the GC Energy Term at 0.131 and 0.022 M Salt Concentration, at Different pH Values[a]

	net charge		center of mass position (Å)		GC (kcal/mol)	
pH	solv	mem	0.131M	0.022M	0.131M	0.022M
1.0	6.9	6.6	22.00 ± 0.14	19.88 ± 0.08	− 5.34 ± 0.08	− 12.66 ± 0.06
2.0	6.6	6.5	21.61 ± 0.14	20.31 ± 0.12	− 5.51 ± 0.08	− 12.53 ± 0.08
3.0	5.7	6.4	19.74 ± 0.08	20.58 ± 0.12	− 6.19 ± 0.06	− 11.82 ± 0.08
4.0	4.1	5.0	22.30 ± 0.12	21.41 ± 0.10	− 4.35 ± 0.06	− 9.38 ± 0.06
5.0	1.1	2.1	23.47 ± 0.10	23.50 ± 0.10	− 2.76 ± 0.04	− 5.05 ± 0.06
6.0	−1.2	0.2	25.03 ± 0.08	25.16 ± 0.08	−1.91 ± 0.04	− 2.75 ± 0.04
7.0	−1.9	−1.4	25.46 ± 0.08	25.47 ± 0.10	−1.28 ± 0.04	− 0.85 ± 0.06
8.0	−2.0	−1.9	25.68 ± 0.08	25.32 ± 0.10	−1.31 ± 0.04	− 0.05 ± 0.06
9.0	−2.0	−2.0	25.62 ± 0.08	25.42 ± 0.08	−1.02 ± 0.04	− 0.23 ± 0.04

[a] Error bars represent twice the standard deviation of the mean.

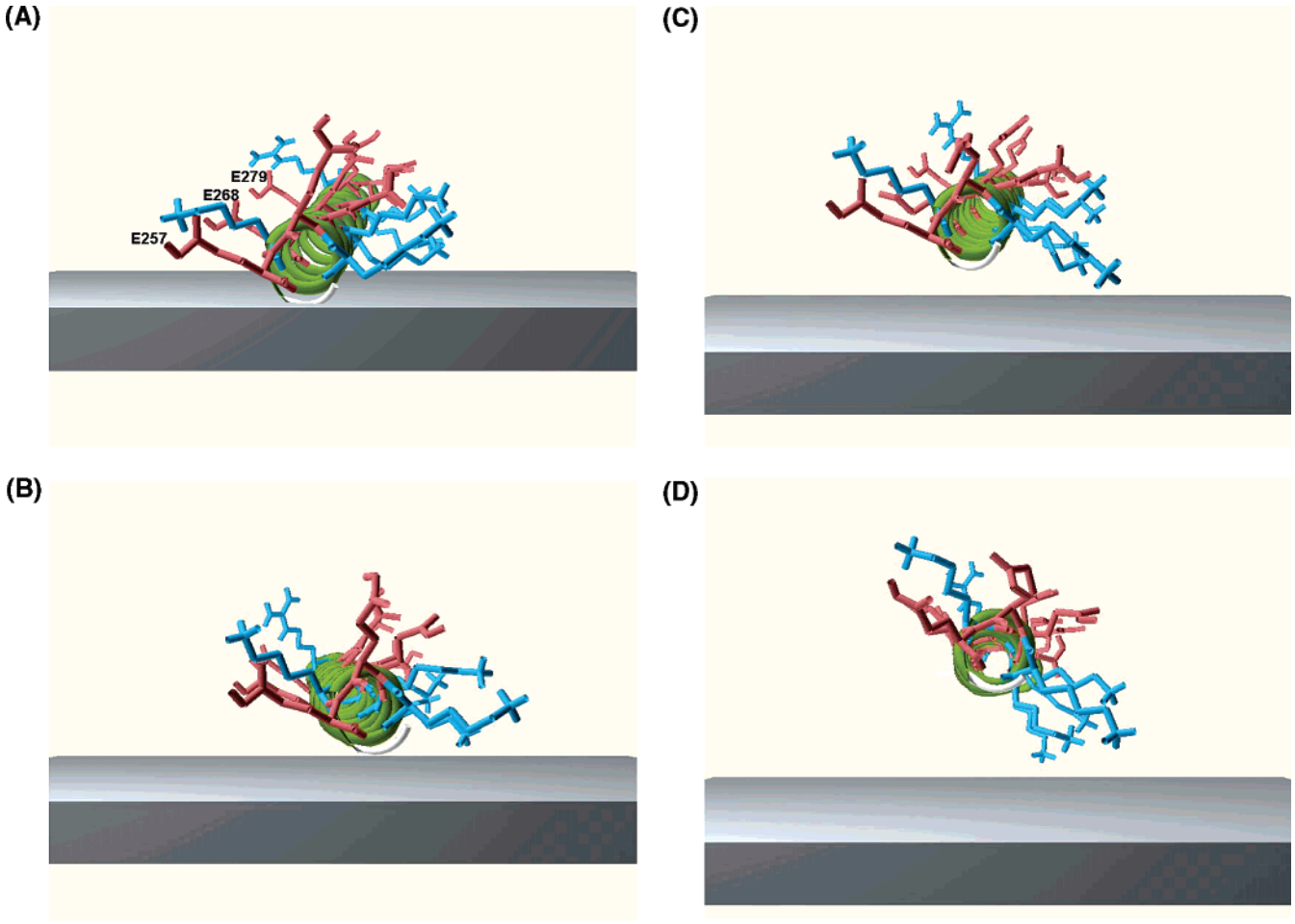

Figure 6. Position of VEEKS (minimized average structure) relative to the membrane at different pH values. The upper surface represents the charge plane (z = 16 Å). The lower surface represents the hydrocarbon/headgroup interface (z = 13 Å). Acidic residues are shown in red, basic residues are in blue. (A) pH = 2.0. The center of mass of the interafacial glutamates is at z_{E257} = 18.4 Å, z_{E268} = 19.5 Å, and z_{E279} = 21.9 Å. (B) pH = 4.0; z_{E257} = 20.7 Å, z_{E268} = 21.2 Å, z_{E279} = 22.8 Å. (C) pH = 5.0; z_{E257} = 22.4 Å, z_{E268} = 23.4 Å, z_{E279} = 25.2 Å. (D) pH = 7.0; z_{E257} = 26.8 Å, z_{E268} = 27.1 Å, z_{E279} = 27.6 Å.

(2) both electrostatic and nonelectrostatic energy contributions are accounted for, and (3) conformational changes due to titration of residues are taken into account. In addition, MD simulations with implicit membrane are much faster than explicit simulations and longer simulation times are more computationally affordable.

Multiple site titration is usually addressed by calculating protonation probabilities without accounting for all ionization states exactly or by using Monte Carlo;[37,72] Tanford and Roxby[73] used a mean-field approximation[21] to calculate the average protonation of a titratable residue using the average charges of the titratable groups. In the reduced-site approximation (RSA),[21] the maximal and minimal protonation free energies are used to fix the ionization state of residues that titrate at pH far from a given pH and thus reduce the number of states explicitly treated. Yang et al. calculated the protonation probabilities by treating all states of the residues within 7 Å radius and by using the Tanford−Roxby approximation for other residues.[22] Gilson developed the so-called cluster method[23] that, as RSA, fixes protonation states of residues that titrate far from a pH of interest and places the other residues into clusters according to the criteria that cluster−cluster interactions are small. It considers all protonation states of residues within a cluster and uses the Tanford−Roxby approximation for cluster−cluster interactions.

Our method divides a protein into clusters of residues that have atoms not more than 9 Å apart from residue *i* (where 9 Å corresponds to the IMM1-GC cutoff distance for van der Waals and electrostatic interactions) and considers all ionization states of residues within a cluster but neglects intercluster interactions.

Both pK_a calculations and protein binding to membranes can be sensitive to which of the two carboxyl oxygens of Glu and Asp residues gets the proton. The protonation should be carried out at each oxygen atom, followed by averaging of the results. Mongan et al. approached the tautomeric state problem by introducing two hydrogens, kept 180° apart by an improper torsion, to each carboxyl oxygen, providing that only one of the four hydrogens can have a nonzero charge.[44] To address different proton tautomers, we added the protein to each site and chose the one that yields lower energy as the probable protonation site. During subsequent MD simulations, the protonation sites did not change, which might affect the conformational sampling. The effects of this approximation should be explored in future studies.

Uncertainties in ΔG Calculation. The calculations significantly underestimate the membrane binding affinity of VEEKS. Given that IMM1-GC gives reasonable values for other peptides,[54] we should consider other factors that could contribute to the discrepancy in the calculated and the experimental ΔG. The first is the effect of the membrane curvature. As a consequence of the larger curvature, lipid packing in SUVs is less ordered and the hydrophobic acyl chains are more exposed, which enhances hydrophobic interactions between lipids and proteins.[66−69] Binding of VEEKS to LUVs is probably ∼10 times weaker than that to SUVs of the same composition,[74] implying that the free energy of binding should be less favorable than that of SUVs, by ∼1.4 kcal/mol. However, this does not fully account for the discrepancy that we observe.

Lipid demixing, i.e., an increase in concentration of anionic lipids at the binding site, can reduce the free energy of binding.[75] It especially comes into effect in the low membrane surface charge density/high protein surface charge density case. Since the "smeared" charge approximation used in the Gouy−Chapman theory cannot capture local charge fluctuations, to quantitatively estimate the effect of lipid demixing on ΔG, we ran simulations at pH = 7.0 with the molar fraction of anionic lipids of 0.5, 0.7, and 1.0 and found that ΔG decreases by up to 1.2 kcal/mol. The effect of lipid demixing on the apparent pK_a of binding would be to shift it to higher pH. However, this effect is also too small to account for the observed discrepancy.

A more important factor could be favorable protein−protein interactions, which is not accounted for in our calculations. Given that the surface area of the peptide is ∼700 Å^2, at the experimental protein/lipid ratio (1/100), which corresponds to 4200 Å^2 per molecule if all peptides are membrane-bound (assuming lipid accessibility of 0.6), the surface concentration of peptide on vesicles is high enough to allow protein−protein interactions. To test whether these interactions would decrease the free energy of binding, we performed simulations of a dimer on the membrane. Two helical VEEKS peptides in the optimal orientation were placed on the membrane surface parallel to each other, 15 Å apart; the simulation protocol was the same as for the monomer, with twice the simulation times. According to the results, basic residues of one helix form salt bridges with acidic residues of the second helix, which lowers the energy by ∼10 kcal/mol. Figure 7 shows a dimer on the membrane after 1.4 ns of MD simulation at pH = 4.0 and minimization. Johnson et al. reported that VEEKS dimerizes in dilute buffer.[76] Dimerization should be more prevalent on the membrane due to higher effective concentrations and would bring about a significant decrease of the free energy of binding. Experimental verification of this hypothesis would be possible by studies at different peptide/lipid ratios.

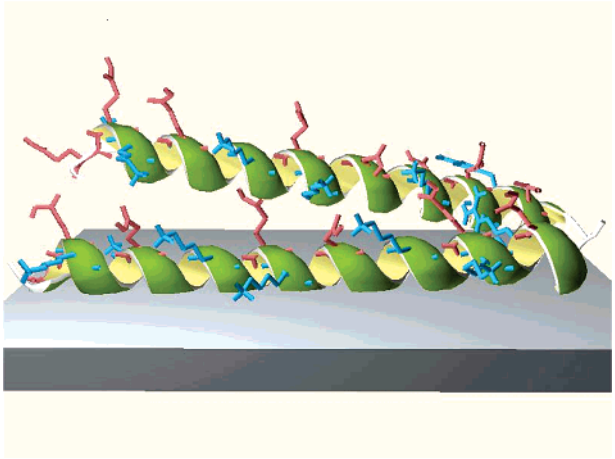

Figure 7. Dimer of VEEKS on the membrane, after 1.4 ns of MD simulation at pH = 4.0 and energy minimization. The center of mass of the dimer is at 21.13 Å. The charge plane and the hydrophobic/hydrophilic interface are represented by the upper and the lower surface, respectively.

A rough estimate of the free energy of binding with dimerization can be obtained as follows. At pH 7.0, the average effective transfer energy per monomer when dimerization takes place is -10.3 ± 0.3 kcal/mol. Given that $-RT \ln(V_b/V_f) = 5.3$ kcal/mol and $-T\Delta S^{\Theta} = 1.1$ kcal/mol and assuming that ΔG_{ion} (pH = 7.0) is the same as for monomer (0.75 kcal/mol) and that the translational/rotational entropy loss due to dimerization is of the same order as that for glycophorin A at 1 M, $-T\Delta S^{dimer} \sim 2.5$ kcal/mol,[77] the free energy of binding per monomer is approximately -0.6 ± 0.3 kcal/mol, which is in good agreement with the measured ΔG.[52] A more accurate estimate of ΔG would require calculation of ΔS^{dimer} at the effective protein concentration on the membrane, taking into account excluded volume effects.

In principle, the translational and rotational entropy loss, ΔS^{Θ}, should be obtained by calculating the probability distribution of positions of the center of mass within the binding distance from the membrane surface and the probability distribution of orientations with respect to the fixed coordinate system attached to the membrane surface.[60] For convenience, we assumed that ΔS^{Θ} is the same as that for pentalysine[60] and hence neglected its dependence on the size of the protein and the strength of binding. Given the weak binding of VEEKS to LUVs, this should be a good approximation.

The transfer effective energy, ΔW_{tr}, is obtained from MD trajectories for the transition from "helix in water" to "helix on the membrane". However, according to CD studies VEEKS is a random coil in solution (with 14% helicity) and adopts an α-helical conformation in the presence of anionic lipids.[64] The free energy of helix formation, $\Delta G_{rc\rightarrow hlx}$, which for the transition from 14% to 100% helicity is ∼1.1 kcal/mol, should thus be added to the overall free energy of binding. That would make the free energy of binding somewhat more positive.

Acknowledgment. We thank Dr. R. Cornell and Dr. M. Gunner for fruitful discussions and comments on the manuscript. This work was supported by the National Science Foundation (MCB-0316667) and a CUNY Collaborative Incentive Grant.

Supporting Information Available: Validation of the pK_a calculations. This material is available free of charge via the Internet at http://pubs.acs.org.

References and Notes

(1) Zwaal, R. F.; Comfurius, P.; Bevers, E. M. *Biochim. Biophys. Acta* **1998**, *1376*, 433.
(2) Huang, M. D.; Rigby, A. C.; Morelli, X.; Grant, M. A.; Huang, G. Q.; Furie, B.; Seaton, B.; Furie, B. C. *Nat. Struct. Biol.* **2003**, *10*, 751.
(3) Reutelingsperger, C. P.; van Heerde, W. L. *Cell. Mol. Life Sci.* **1997**, *53*, 527.
(4) Tucker, W. C.; Chapman, E. R. *Biochem. J.* **2002**, *366*, 1.
(5) Bruhn, H.; Riekens, B.; Berninghausen, O.; Lieppe, M. *Biochem. J.* **2003**, *375*, 737.
(6) Stenger, S.; Hanson, D. A.; Teitelbaum, R.; Dewan, P.; Niazi, K. R.; Froelich, C. J.; Ganz, T.; Thoma-Uszynski, S.; Melian, A.; Bogdan, C.; Porcelli, S. A.; Bloom, B. R.; Krensky, A. M.; Modlin, R. L. *Science* **1998**, *282*, 121.
(7) Westerhoff, H. V.; Juretic, D.; Hendler, R. W.; Zasloff, M. *Proc. Natl. Acad. Sci. U.S.A.* **1989**, *86*, 6597.
(8) Zasloff, M. *Nature* **2002**, *415*, 389.
(9) Benech, R. O.; Kheadr, E. E.; Lacroix, C.; Fliss, I. *Appl. Environ. Microbiol.* **2002**, *68*, 5607.
(10) Sato, T. K.; Overduin, M.; Emr, S. D. *Science* **2001**, *294*, 1881.
(11) Cho, W.; Stahelin, R. V. *Annu. Rev. Biophys. Biomol. Struct.* **2005**, *34*, 119.
(12) Behrisch, A.; Dietrich, C.; Noegel, A. A.; Schleicher, M.; Sackmann, E. *Biochemistry* **1995**, *34*, 15182.
(13) Hanakam, F.; Gerisch, G.; Lotz, S.; Alt, T.; Seelig, A. *Biochemistry* **1996**, *35*, 11036.
(14) O'Brien, J.; Kishimoto, Y. *FASEB J.* **1991**, *5*, 301.
(15) Kishimoto, Y.; Hiraiwa, M.; O'Brien, J. S. *J. Lipid Res.* **1992**, *33*, 1255.
(16) Fürst, W.; Sandhoff, K. *Biochim. Biophys. Acta* **1992**, *1126*, 1.
(17) de Alba, E.; Weiler, S.; Tjandra, N. *Biochemistry* **2003**, *42*, 14729.
(18) Bollinger, J. G.; Diraviyam, K.; Ghomashchi, F.; Murray, D.; Gelb, M. *Biochemistry* **2004**, *43*, 13293.
(19) Warshel, A. *Biochemistry* **1981**, *20*, 3167.
(20) Bashford, D.; Karplus, M. *Biochemistry* **1990**, *29*, 10219.
(21) Bashford, D.; Karplus, M. *J. Phys. Chem.* **1991**, *95*, 9556.
(22) Yang, A. S.; Gunner, M. R.; Sampogna, R.; Sharp, K.; Honig, B. *Proteins* **1993**, *15*, 252.
(23) Gilson, M. K. *Proteins* **1993**, *15*, 266.
(24) Antosiewicz, J.; McCammon, J. A.; Gilson, M. K. *J. Mol. Biol.* **1994**, *238*, 415.
(25) Sham, Y. Y.; Chu, Z. T.; Warshel, A. *J. Phys. Chem. B* **1997**, *101*, 4458.
(26) Wlodek, S. T.; Antosiewicz, J.; McCammon, J. A. *Protein Sci* **1997**, *6*, 373.
(27) van Vlijmen, H. W. T.; Schaefer, M.; Karplus, M. *Proteins* **1998**, *33*, 145.
(28) Mehler, E. L.; Guarnieri, F. *Biophys. J.* **1999**, *75*, 3.
(29) Sandberg, L.; Edholm, O. *Proteins* **1999**, *36*, 474.
(30) Dlugosz, M.; Antosiewicz, J. M. *Phys. Rev. E* **2004**, *69*, 021915.
(31) Sharp, K. A.; Honig, B. *J. Phys. Chem.* **1990**, *94*, 7684.
(32) Honig, B.; Sharp, K.; Yang, A.-S. *J. Phys. Chem.* **1993**, *97*, 1101.
(33) Honig, B.; Nicholls, A. *Science* **1995**, *268*, 1144.
(34) Ben-Tal, N.; Honig, B.; Peitzsch, R. M.; Denisov, G.; McLaughlin, S. *Biophys. J.* **1996**, *71*, 561.
(35) Beroza, P.; Fredkin, D. R. *J. Comput. Chem.* **1996**, *17*, 1229.
(36) Im, W.; Bernèche, S.; Roux, B. *J. Chem. Phys.* **2001**, *114*, 2924.
(37) Georgescu, R. E.; Alexov, E. G.; Gunner, M. R. *Biophys. J.* **2002**, *83*, 1731.
(38) Bashford, D.; Case, D. A. *Annu. Rev. Phys. Chem.* **2000**, *51*, 129.
(39) Beveridge, D. L.; DiCapua, F. M. *Annu. Rev. Biophys. Biophys. Chem.* **1989**, *18*, 431.
(40) Warshel, A.; Sussman, F.; King, G. *Biochemistry* **1986**, *25*, 8368.
(41) Kollman, P. *Chem. Rev.* **1993**, *93*, 2395.
(42) Simonson, T.; Carlsson, J.; Case, D. A. *J. Am. Chem. Soc.* **2004**, *126*, 4167.
(43) Baptista, A. M.; Teixeira, V. H.; Soares, C. M. *J. Chem. Phys.* **2002**, *117*, 4184.
(44) Mongan, J.; Case, D. A.; McCammon, J. A. *J. Comput. Chem.* **2004**, *25*, 2038.
(45) Lee, M. S.; Salsbury, F. R. Jr.; Brooks, C. L., III *Proteins* **2004**, *56*, 738.
(46) Khandogin, J.; Brooks, C. L. III *Biophys. J.* **2005**, *89*, 141.
(47) Sharp, K. A. *Proteins* **1998**, *33*, 39.
(48) Misra, V. K.; Hecht, J. L.; Yang, A.-S.; Honig, B. *Biophys. J.* **1998**, *75*, 2262.
(49) Alexov, E. *Proteins* **2004**, *56*, 572.
(50) Kalmar, G. B.; Kay, R. J.; Lachance, A.; Aebersold, R.; Cornell, R. B. *Proc. Natl. Acad. Sci. U.S.A.* **1990**, *87*, 6029.
(51) MacDonald, J. I. S.; Kent, C. *Protein Expression Purif.* **1993**, *4*, 1.
(52) Johnson, J. E.; Xie, M.; Singh, L. M. R.; Edge, R.; Cornell, R. B. *J. Biol. Chem.* **2003**, *278*, 514.
(53) Brooks, B. R.; Bruccoleri, R. E.; Olafson, B. D.; States, D. J.; Swaminathan, S.; Karplus, M. *J. Comput. Chem.* **1983**, *4*, 187.
(54) Lazaridis, T. *Proteins* **2005**, *58*, 518.
(55) Neria, E.; Fischer, S.; Karplus, M. *J. Chem. Phys.* **1996**, *105*, 1902.
(56) McLaughlin, S. *Annu. Rev. Biophys. Biophys. Chem.* **1989**, *18*, 113.
(57) Berg, J. M.; Tymoczko, J. L.; Stryer, L. *Biochemistry*, 5th ed.; W. H. Freeman & Company: New York, 2002.
(58) Lazaridis, T.; Karplus, M. *Proteins* **1999**, *35*, 133.
(59) Lazaridis, T. *Proteins* **2003**, *52*, 176.
(60) Ben-Tal, N.; Honig, B.; Bagdassarian, C. K.; Ben-Shaul, A. *Biophys. J.* **2000**, *79*, 1180.
(61) Victor, K. G.; Cafiso, D. S. *Biophys. J.* **2001**, *81*, 2241.
(62) Nosé, S. A. *J. Chem. Phys.* **1984**, *81*, 511.
(63) Hoover, W. G. *Phys. Rev. A* **1985**, *31*, 1695.
(64) Johnson, J. E.; Cornell, R. B. *Biochemistry* **1994**, *33*, 4327.
(65) Dunne, S. J.; Cornell, R. B.; Johnson, J. E.; Glover, N. R.; Tracey, A. S. *Biochemistry* **1996**, *35*, 11975.
(66) Gazzara, J. A.; Phillips, M. C.; Lund-Katz, S.; Palgunachari, M. N.; Segrest, J. P.; Anantharamaiah, G. M.; Rodrigueza, W. V.; Snow, J. W. *J. Lipid Res.* **1997**, *38*, 2147.
(67) Wieprecht, T.; Apostolov, O.; Seelig, J. *Biophys. Chem.* **2000**, *85*, 187.
(68) Wieprecht, T.; Beyermann, M.; Seelig, J. *Biophys. Chem.* **2002**, *96*, 191.
(69) Chenal, A.; Vernier, G.; Savarin, P.; Bushmarina, N. A.; Geze, A.; Guillain, F.; Gillet, D.; Forge, V. *J. Mol. Biol.* **2005**, *349*, 890.
(70) Masunov, A.; Lazaridis, T. *J. Am. Chem. Soc.* **2003**, *125*, 1722.
(71) Mottamal, M.; Zhang, J.; Lazaridis, T. *Proteins*, published online January 4, 2006.
(72) Beroza, P.; Fredkin, D. R.; Okamura, M. Y.; Feher, G. *Proc. Natl. Acad. Sci. U.S.A.* **1991**, *88*, 5804.
(73) Tanford, C.; Roxby, R. *Biochemistry* **1972**, *11*, 2192.
(74) Cornell, R. B. Simon Fraser University. Personal communication, 2005.
(75) May, S.; Harries, D.; Ben-Shaul, A. *Biophys. J.* **2000**, *75*, 1747.
(76) Johnson, J. E.; Rao, N. M.; Hui, S. W.; Cornell, R. B. *Biochemistry* **1998**, *37*, 9509.
(77) Zhang, J.; Lazaridis, T. *Biophys. J.*, submitted for publication.